AN EXPERIMENTAL STUDY TO INVESTIGATE HYPERVELOCITY IMPACTS ON PRESSURE VESSELS

F. Schäfer, E. Schneider

Ernst-Mach-Institut - Fraunhofer Institut für Kurzzeitdynamik
Eckerstr. 4, D-79104 Freiburg

M. Lambert

ESA-ESTEC
Postbus 299, NL-2200 AG Noordwijk, The Netherlands

ABSTRACT

Thin-walled cylindrical gas-filled pressure vessels made of aluminium alloy and unalloyed titanium were impacted by hypervelocity aluminium projectiles. Impact velocity was fixed at 7 km/s, projectile sizes ranged up to 4.9 mm for the Al-vessels, and up to 10 mm for the Ti-vessels. The pressure was varied up to roughly 95% of the experimental static burst pressure. The loading conditions that lead to catastrophic rupture were established. It was found that at high hoop stresses the amount of kinetic energy needed to rupture the vessel is low whereas at low wall stresses large impact energies are required to cause catastrophic rupture. In some experiments crack propagation started in the impact hole, which is a failure mode for gas-filled pressure vessels that has not been reported before. A few experiments involved shielded vessels. It was demonstrated that shielding may prevent catastrophic rupture.

1. INTRODUCTION

Post flight investigations of impact damages produced by particle impacts in missions like EURECA (European Retrievable Carrier), LDEF (Long Duration Exposure Facility), HST (Hubble Space Telescope) [1] and even the Space Shuttle proved considerable particle fluxes in the Low Earth Orbit (LEO). While there has been a considerable experimental and numerical effort to analyze and simulate impact damages of all kinds of non-pressurized spacecraft structures which has indeed led to better understanding of impact mechanisms and resulted in effective design countermeasures, there has been little effort to consider pressurized modules.

Any spacecraft needs pressure vessels onboard. Considering for example an Attitude and Orbit Control System (AOCS), two types of pressure vessels are necessary: Firstly, vessels containing the propellant for the AOCS under low pressure, which feed the thrust engines and secondly, vessels filled with an inert gas (helium, nitrogen) under high pressure, which are used to keep the pressure in the propellant tank at the adequate level for firing the attitude control thrust engines. Whenever such tanks are attached to the outer spacecraft wall they are exposed directly to the micrometeoroid and debris environment of their orbit.

The risks emanating from a debris impact on any kind of stressed container cannot be underestimated, as was shown in studies conducted by NASA [2,3,4]: Impact damages ranged from simple vessel perforation to catastrophic rupture of the vessels. Thus, besides the failure of the vessel, large wall fragments can result that propagate at low velocities and pose an excess hazard to other spacecraft components in the vicinity of the impacted tank.

2. PURPOSE OF THE STUDY

The purpose of this study was the experimental determination of impactor energies at hypervelocity and corresponding vessel pressures that lead to catastrophic failure of a cylindrical vessel model, and the effect of a protection bumper shield placed in front of the vessel. Hypervelocity impact damages were to be investigated systematically.

3. OVERVIEW OF EFFECTS RELATED TO HYPERVELOCITY IMPACTS ON PRESSURE VESSELS

3.1 Unpressurized vessel

When an aluminium projectile encounters a thin metal bumper plate in the upper hypervelocity regime around 7 km/s, the shock pressures generated in the projectile and the plate are sufficiently high to fracture and partly melt projectile and bumper material [5]. The projectiles kinetic energy is reduced and the fragments are spread radially. At constant impact velocity, the projectile diameter to bumper thickness ratio governs the fragment

size distribution. A detailed analysis of such d/t effects is presented in [6]. During front wall perforation, lateral shock waves are produced in the plate which damp out quickly to compression waves. Considering a vessel, those waves propagating in circumferential direction may interfere at the vessels rear side and exceed the material strength. Rear wall impact damages include cratering, spallation, perforation, bulging, petalling, etc., see e.g. [6].

3.2 Pressurized vessel

If the vessel is filled with gas, some different damage mechanisms arise from the presence of wall stresses and the interaction of the fragment cloud with pressure gas:

- Stress concentration around the impact hole can induce front side failure
- Ablation and deceleration mechanisms reduce the kinetic energy of the fragments. Under certain conditions, the fragments energy can be completely consumed up [7]
- Rear wall cratering and perforation of the fragments can initiate crack growth due to stress magnification and cause subsequently rear side failure
- Shockwaves are transmitted from the projectile-target interface into the pressure gas. Bow waves of the individual fragments add up to a strong gas-shockwave, which impacts the rear wall and can cause rear side failure
- A combination of all processes is possible

At this point, a clear definition of 'catastrophic failure' has to be given which is among others necessary to unambiguously perform an analysis of the results: The criterion for 'catastrophic failure' of a pressure vessel subjected to hypervelocity impact is met, if there exists at least one axial crack that is equal or larger than the vessels axial length.

4. MATERIALS AND TEST SAMPLES

The test samples were cylindrical vessels, with a wall thickness of 1 mm, a length of 350 mm and a diameter of 150 mm.

The material tested in the first phase of the study was Al 5754 (AlMg3), an aluminium magnesium alloy with a moderate strength of 260 MPa, an elongation of 8% and a fracture toughness of 60-80 MPa$\sqrt{m}$. Aluminium-magnesium alloys have a good specific strength and a low density among aluminium alloys. They are used for storage tanks and pressure vessels [8]. Al 5754 was available in drawn tube form. The aluminium vessels were manufactured by welding caps to the tube ends and machining down the wall to the final thickness of nominally 1.0 mm. The manufacturing process introduced local wall thickness variations of up to 20%. The thickness variations of the vessels was accounted for by error bars in the analysis.

Restricted by the budget of the study, the titanium vessels were made of 1 mm uniformly thick sheets. However, little influence of the axial weld on the hypervelocity impact results was expected, because weldment factors for titanium are generally above 0.85. The material selected was unalloyed titanium of ASTM grade 2, with a strength of 480 MPa, an elongation of 32% and a fracture toughness of ca. 66 MPa$\sqrt{m}$ [9]. Titanium grade 2 is widely used in industrial applications, having a moderate strength among the titanium alloys, with an excellent formability and a good ductility.

5. QUASI-STATIC INFLATION TESTS

Quasi-static inflation tests were conducted for both materials prior to the impact tests. The burst pressure of vessels is influenced by a number of factors such as the quality of the axial and circumferential welds and wall thickness variations which are introduced by the manufacturing process, strain rate sensitivity of the material, material inhomogeneities (e.g. voids, inclusions etc.) and others.

The burst pressures recorded will be referred to as 'reference' burst pressures. Wall stresses are normalized by the corresponding maximum wall stresses and are denoted 'effective' wall stresses.

Two quasi-static inflation experiments were conducted on Al 5754 vessels. At inflation rates of around 0.3 bar/s, the burst pressures were 22.5 bar and 25.6 bar. Wall thickness measurements at different locations on the vessels revealed that the thinnest points were 0.9 mm and 1.0 mm, respectively. For the analysis of the hypervelocity impact results the latter static burst pressure was taken as the reference burst pressure.

Burst pressures recorded from quasi-static inflation tests of 3 titanium vessels were 75.9 bar, 73.7 bar and 74.2 bar, where inflation rates ranged between 0.1 bar/s and 1.3 bar/s. As was expected, the fracture pattern of all vessels showed also one crack along the axial welding joints. To ensure that the welding joint didn't affect the results of the hypervelocity impact tests, the vessels were placed in the target chamber such that the welding joint was not impactecd by projectile or fragments. The reference burst pressure for titanium vessels was chosen the arithmetic mean of all test results, i.e. 74.6 bar.

6. HYPERVELOCITY IMPACTS ON PRESSURE VESSELS - EXPERIMENTAL STUDY

For experimental micrometeoroid and debris simulation three hypervelocity impact test facilities are available at Ernst-Mach-Institut. The operation principle of this type of accelerator has first been described by Crozier and Hume in 1957 [10]. The EMI light gas gun accelerators are described by Stilp [11].

6.1 Unshielded vessels

All projectiles were aluminium spheres made of Al 1098 and Al 2017, impacting with a velocity of around 7 km/s at normal incidence in the center of the vessels cylinder wall.

Projectile diameters involved in the aluminium vessels test program ranged from 2 mm to 4.9 mm, at impact velocities between 6.6 km/s and 7.5 km/s, having a kinetic energy of 260 J to 4150 J. Inflation pressures ranged between 1.8 bar and 24.6 bar, i.e. 7 % and 96 % of the reference burst pressures.

The titanium pressure vessels were impacted by spheres between 5 mm and 10 mm diameter at impact velocities ranging from 6.1 km/s to 7.5 km/s. Thus kinetic impact energies were roughly one order of magnitude higher than for the aluminium vessels, namely between 4 kJ and 36 kJ. Inflation pressures ranged here from 9.3 bar to 61.4 bar, thus 12 % and 82 % of the reference pressure. The test matrices for both materials are provided in Chapter 10.
A fully equipped and fixed vessel, placed in the target chamber is shown in Fig. 1.

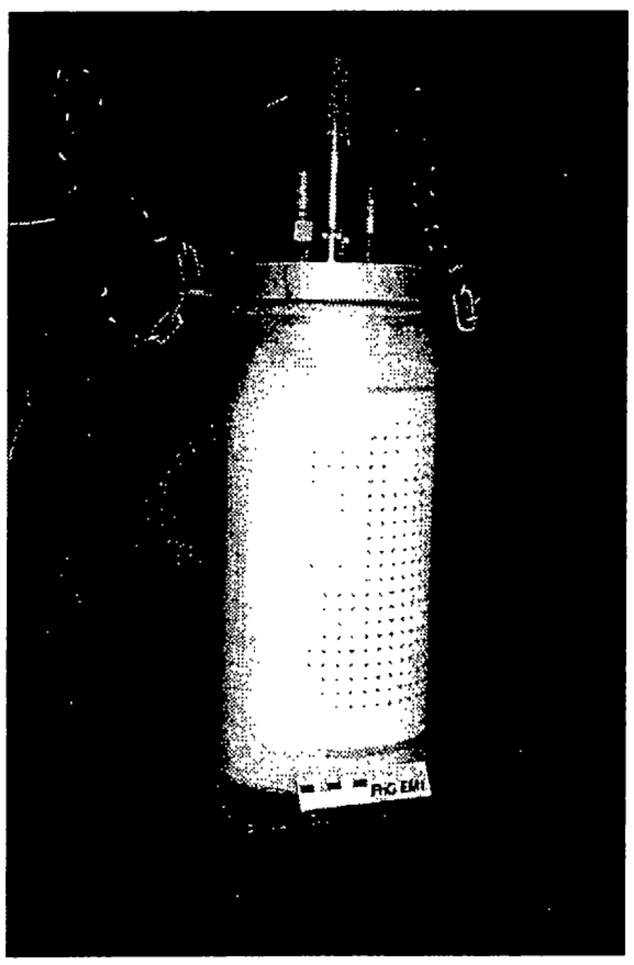

Figure 1. Fully equipped vessel, placed in the target chamber

To determine the parameters that result in catastrophic rupture, for a given kinetic energy the vessel pressure was increased in subsequent tests until catastrophic failure occurred. This was done for several energy levels. Variation of kinetic energy was realized by variation of projectile diameters.

The impact energy ranges as used in the following are distinguished by the overall damages to the impacted vessels. Three ranges are established, which are a strong function of the materials used:

- Low kinetic energy is referred to here as energy levels which caused minor rear side damage.
- The medium energy range is distinguished by rear wall cratering, bulging and front side burst; all damage features being a function of increasing vessel pressure.
- In the high kinetic impact range, in general, severe rear side damage such as perforation and petalling has occurred, leading at increased pressures to failure from the rear side.

6.1.1 Low kinetic energy

At low pressures close to vacuum, impact damages are similar to a simple double bumper system of thin plates (Whipple shield). Impact damages at the rear wall of the vessel are low, at the most small craters, tiny bulges and spallations are produced by the fragments impact. In experiment Al-1 involving a 2 mm sphere at 6.7 km/s and a pressure of 2.0 bar (wall stress of 0.08), just tiny craters were found on the vessels back wall. At slightly higher pressure levels, no noticeable damage to the rear wall was observed due to the enhanced interaction between fragments and pressure gas, which resulted in

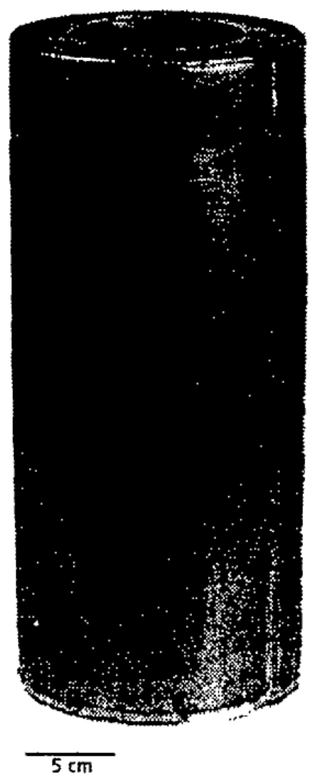

Figure 2. Exp. Ti-1 (front view)
d=5.0 mm, v=6.9 km/s
p=30.3 bar, σ/σ_{max}=0.41

ablation and deceleration of the fragments. This was observed in experiments Al-2 and Al-3 at increased pressures of 6.0 bar and 10 bar (wall stresses of 0.23 and 0.39).

Similarly no rear side damage was produced in experiment Ti-1 (Fig. 2), where an aluminium sphere with a diameter of 5 mm impacted the titanium vessel pressurized to 30.3 bar (wall stress of 0.41).

6.1.2 Medium kinetic energy

As the projectile diameter is increased, larger fragments are produced. Vessel pressures were chosen such, that no fragment impact on the rear side occurred in Exp. Al-9 (4.1 mm sphere, 6.6 km/s, 8.4 bar, wall stress 0.33), and Exp. Ti-5 (8.0 mm sphere, 7.5 km/s, 16 bar, wall stress 0.21), see Fig. 2. In both experiments, the rear wall was strongly bulged outwards due to the strong gas shockwave. No craters were found on the rear wall. These energy levels are still not high enough to initiate cracks at the rear side, at the same time wall stresses are not sufficient to start rupture at the impact hole.

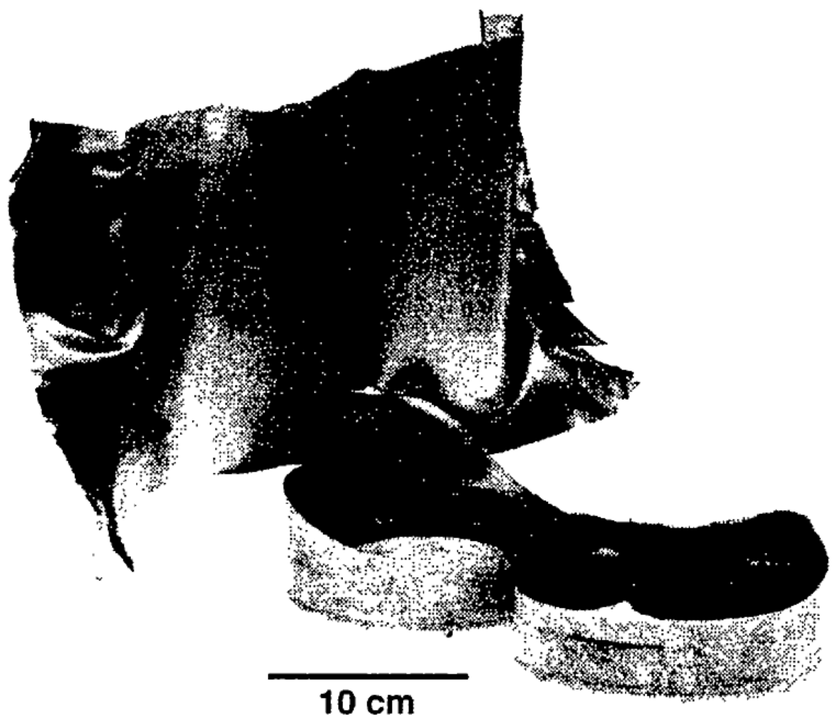

Figure 3. Exp. Al-10 (front view)
d=4.1 mm, v=6.8 km/s
p=11.7 bar, σ/σ_{max}=0.46

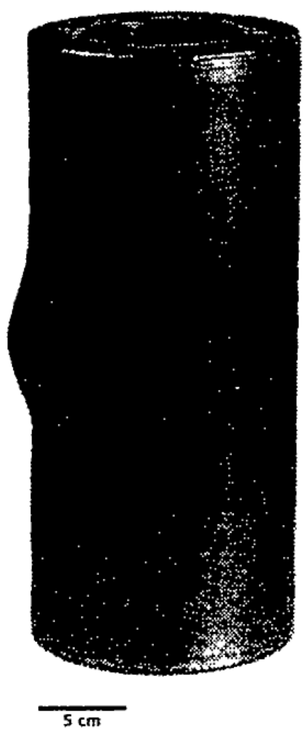

Figure 2. Exp. Ti-5 (rear view)
d=8.0 mm, v=7.5 km/s
p=16 bar, σ/σ_{max}=0.21

In the upper pressure regime at medium kinetic energies stress concentration around the impact hole is sufficient to induce crack growth from the rim of the impact hole. Four experiments involving aluminium vessels (Al-8, Al-10, Al-14 and Al-15) were clearly identified as front side bursts. Stress levels varied between 0.46 and 0.63, the impacting projectiles had a diameter of 4.1 mm and 4.4 mm at velocities between 6.8 km/s and 7.3 km/s. In one of the experiments the vessel wall remained in one piece (see Fig. 3), the others were disintegrated into several large pieces, including unzipping of the vessel

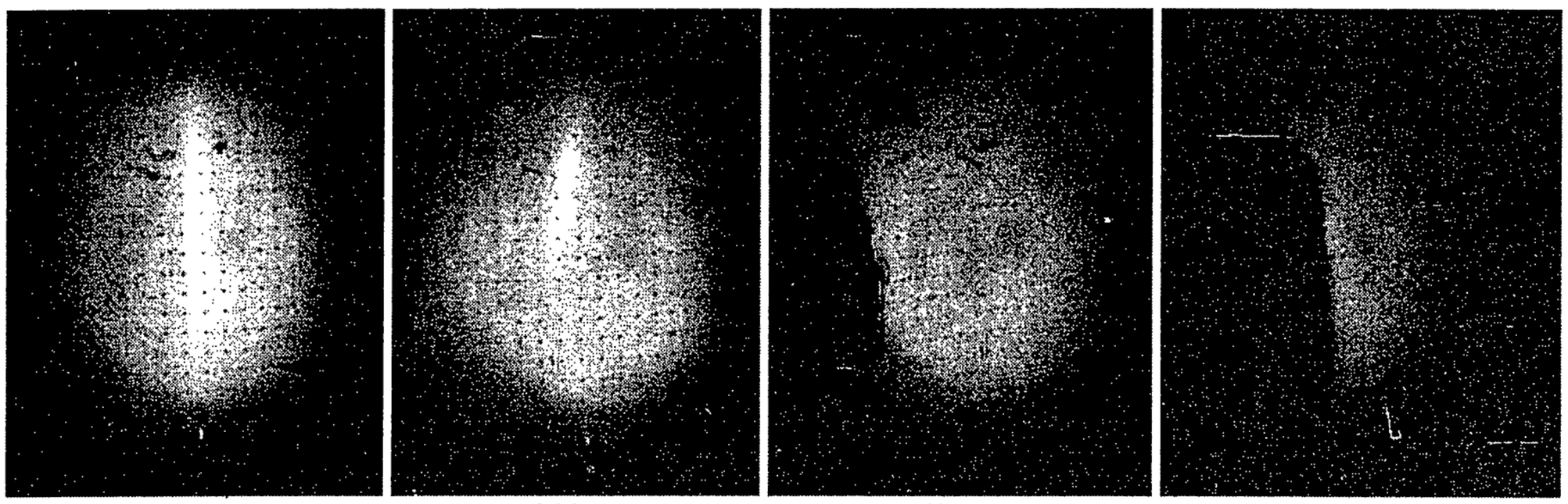

Figure 4. Front side burst recorded with a high speed camera
Exp. Al-10 (side view); d=4.1 mm, v=6.8 km/s; p=11.7 bar, σ/σ_{max}=0.46

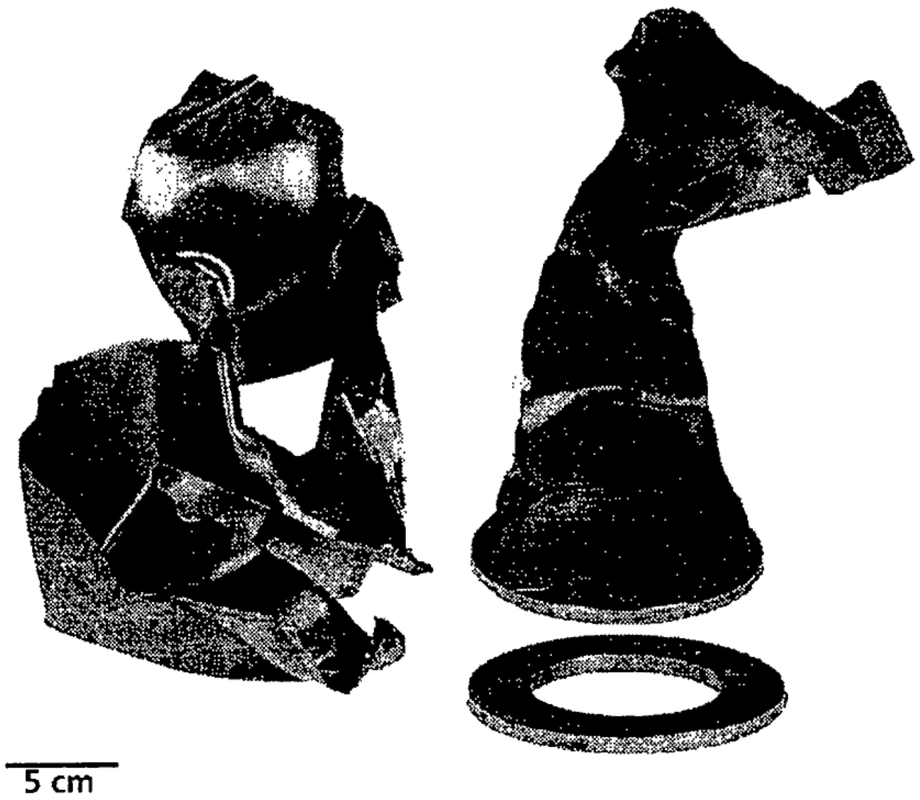

Figure 5. Exp. Ti-7 (front view)
d=8.0 mm, v=7.0 km/s
p=54.4 bar, σ/σ_{max}=0.73

end plates. In experiments No. Al-10 and Al-15 the rupturing was captured by means of a high-speed rotating drum-camera with a copper vapour laser stroboscope as light source. Pictures of Exp. Al-10 are presented in Fig. 4. Time of break-up after impact in three front side bursts of aluminium vessels was several milliseconds after impact. Up to now, there exists no explanation for this long time delay.

This mode of failure was also observed in Exp. Ti-7 (Fig. 5), involving a 8.0 mm diameter sphere impacting at 7.0 km/s the titanium vessel at a wall stress of 0.73.

6.1.3 High kinetic energy

For pressures close to vacuum, severe rear wall damages were observed. In Exp. Al-16 and Al-17 (Fig. 6) at pressures of 1.8 bar and 2.9 bar (wall stresses of 0.07 and 0.11) and projectile diameters of 4.9 mm at 6.9 km/s, the damaged vessels showed similar impact damages: the rear wall was perforated, bulged and petalled by some large remnants of the fragment cloud.

Increasing wall stress leads to catastrophic rupture at the rear side of the vessel. In Exp. Al-18 (Fig. 7) and Al-19 (Fig. 9), both projectile diameters were 5.0 mm, impacting at roughly 7 km/s. Wall stresses amounted to 0.17 and 0.71. Both vessels failed from the rear side. At a wall stress of 0.17, still traces of impact craters were found, which most likely initiated the cracks. Although two large cracks formed, the vessel stayed in one piece. At a wall stress of 0.71, crack growth was not stopped in the wall, the vessel disintegrated into several pieces. No traces of particle impact on the rear side were found.

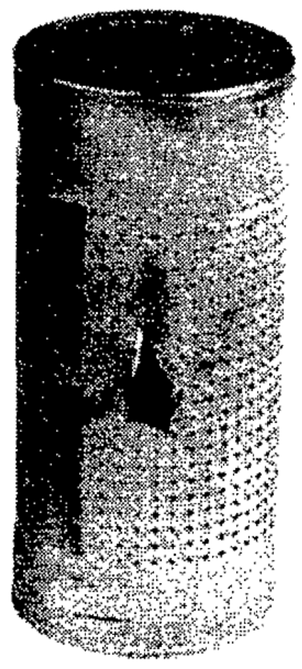

Figure 6. Exp. Al-17 (rear view)
d=4.9 mm, v=6.9 km/s
p=2.9 bar, σ/σ_{max}=0.11

Figure 7. Exp. Al-18 (rear view)
d=4.9 mm, v=6.9 km/s
p=4.3 bar, σ/σ_{max}=0.17

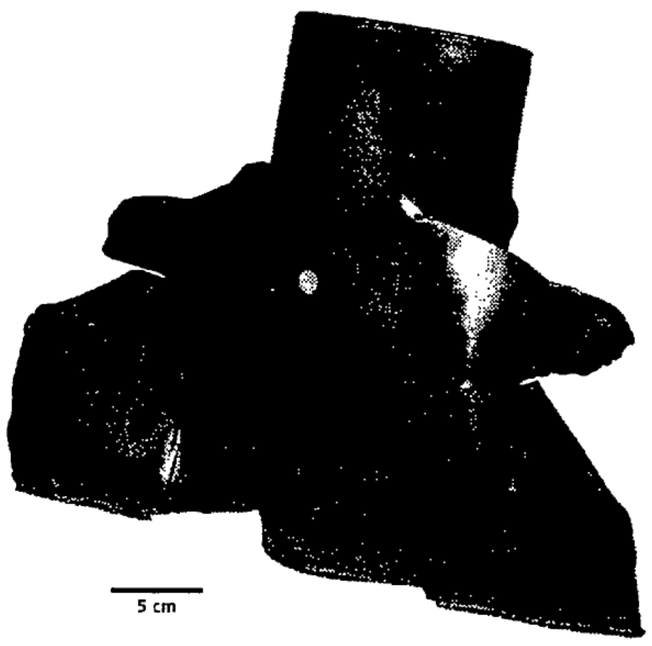

Figure 8. Exp. Ti-8 (front view)
d=8.9 mm, v=7.1 km/s
p=23.4 bar, σ/σ_{max}=0.31

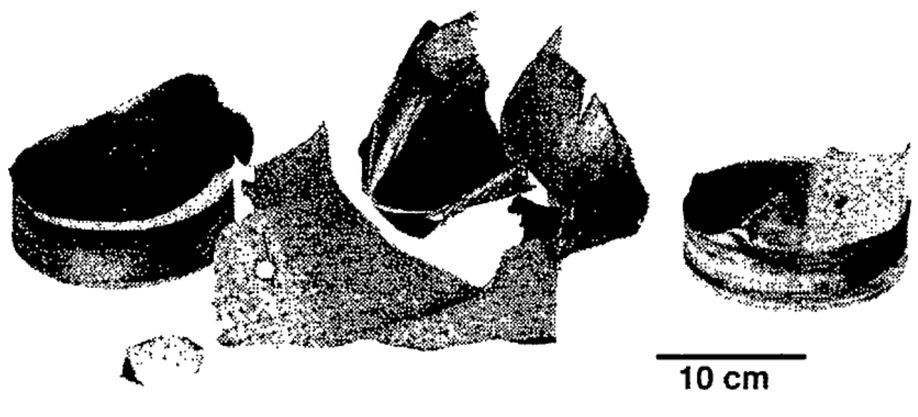

Figure 9. Exp. Al-19
d=4.9 mm, v=7.0 km/s
p=18.3 bar, σ/σ_{max}=0.71

Figure 10. Exp. Ti-10
d=10 mm, v=6.8 km/s
p=55.7 bar, σ/σ_{max}=0.75

Similar features have been observed with titanium vessels in Exp. Ti-9, Ti-8 (Fig. 8) and Ti-10 (Fig. 10), that were stressed to 0.12, 0.31, and 0.75. Projectile diameters here amounted to 8.9 mm and 10.0 mm at impact velocities of between 6.8 km/s and 7.1 km/s. The overall number of wall fragments depended strongly on the wall stress. At the lower wall stresses of 0.12 and 0.31, crack growth was stopped in the vessel wall, whereas for 0.75 the vessel was ruptured into several large pieces.

6.2 Shielded vessels

Four experiments involved shielded experiments to assess the protection efficiency of a shield. The effect of a thin shield is to absorb a fraction of the projectiles' kinetic energy, to fragment the projectile and to distribute the fragments over a large area. In the vessel wall, the cloud produces a large circular secondary impact hole. The shields were 0.5 mm thick plates of Al5754 and 1 mm thick plates of titanium of ASTM grade 2, placed 75 mm in front of the aluminium and

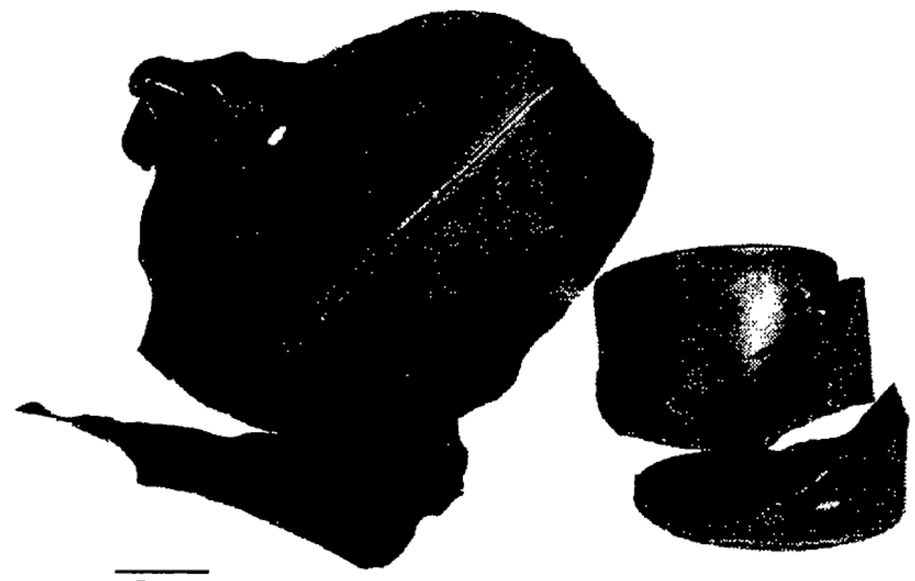

Figure 11. Exp. Ti-6
d=8 mm, v=7.0 km/s
p=30.2 bar, σ/σ_{max}=0.40

titanium vessels, respectively.

The purpose of the aluminium vessels was to investigate if a large perforation hole in the front wall leads to front side failure of the vessel. In the case of the titanium vessels, impact parameters were chosen to be the same as in two experiments where test parameters lead to catastrophic rupture.

Secondary front wall impact holes of 36 and 33 mm diameter were produced in the aluminium vessel tests No. Al-20 and Al-21 by 5 mm and 6 mm projectiles impacting the shield at 6.4 km/s and 5.7 km/s, respectively. Despite vessel pressures of 11 bar in both cases, i.e. wall stresses of approximately 0.4, none of the vessels failed.

Test No. Ti-6 (Fig. 11) was the reference experiment for the first shielded titanium vessel experiment (No. Ti-11,

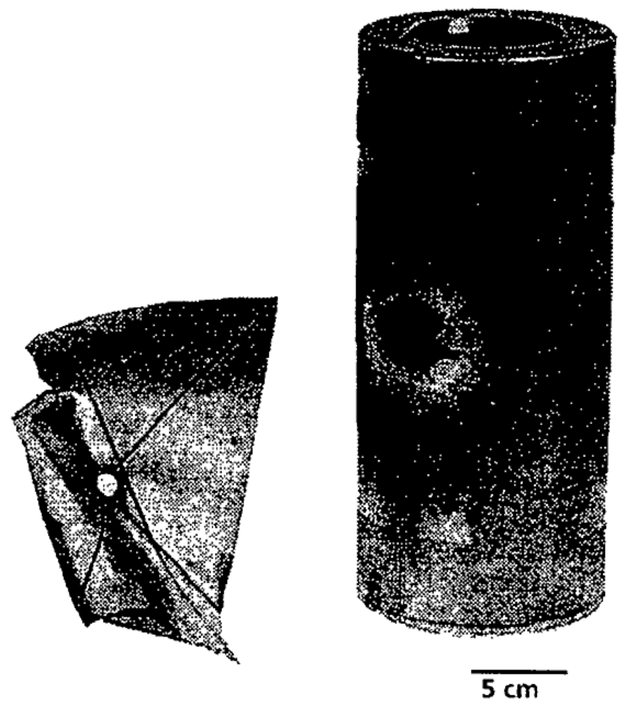

Figure 12. Exp. Ti-11(front view)
shield: titanium 1.0 mm, spacing 75 mm
d=8 mm, v=7.2 km/s
p=30.5 bar, σ/σ_{max}=0.41

see Fig. 12), which had resulted in a catastrophic failure initiated at the rear wall. The projectile involved was an aluminium sphere of 8 mm diameter, impacting at 7.2 km/s, the vessel pressure was 30 bar (wall stress of 0.4). Despite a large secondary impact hole of 45 mm diameter the vessel didn't rupture. However, in the second experiment No. Ti-12 involving a 10 mm projectile at 6.8 km/s and a pressure of 61.4 bar (wall stress ratio of 0.82), the shield could not prevent catastrophic rupture.

7. ANALYSIS

In Fig. 13 a/b and Fig. 14, all results are compiled in a diagram with the normalized wall stresses as abscissa and the projectile kinetic energy as ordinate. Error bars account for uncertainties in wall thickness and associated wall stresses in Fig. 3a. The experimental results are divided into 'catastrophic' and 'non-catastrophic'. The borderline that separates the

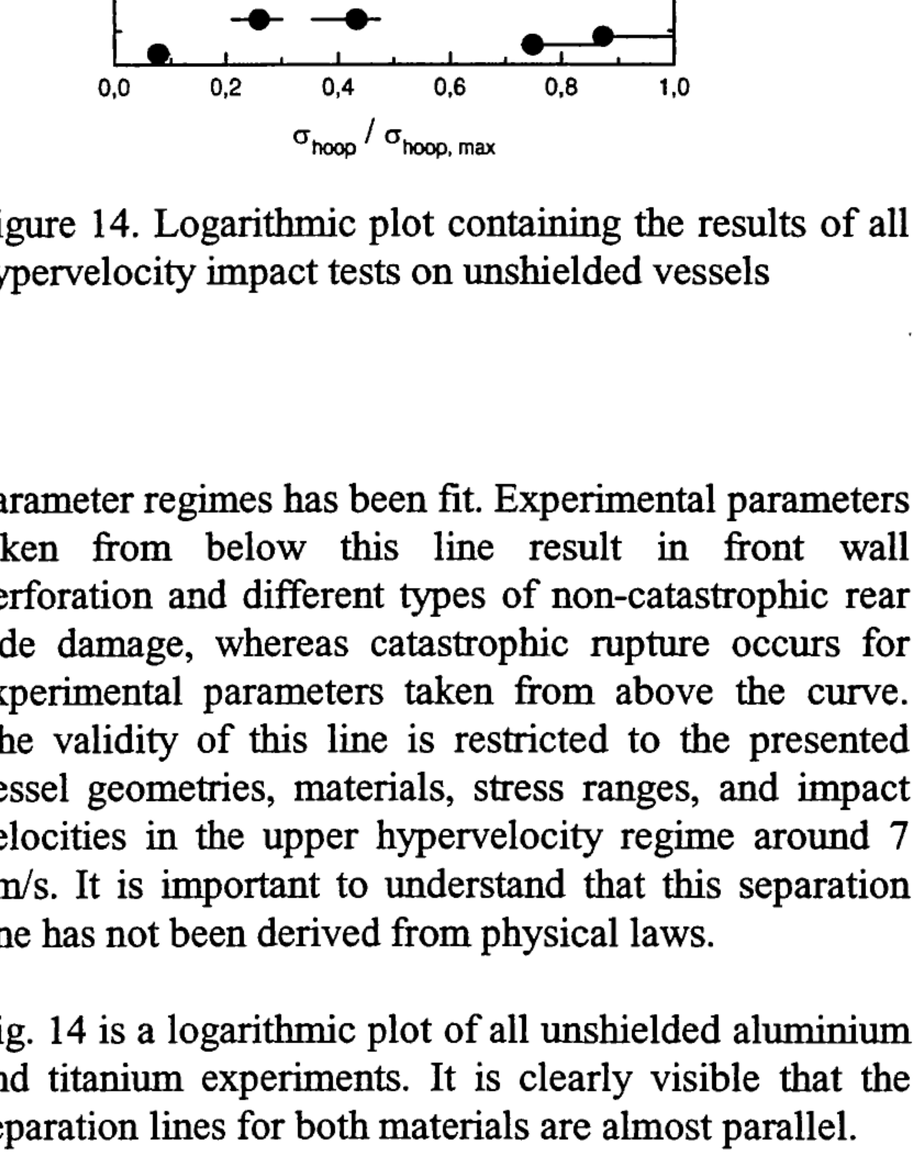

Figure 14. Logarithmic plot containing the results of all hypervelocity impact tests on unshielded vessels

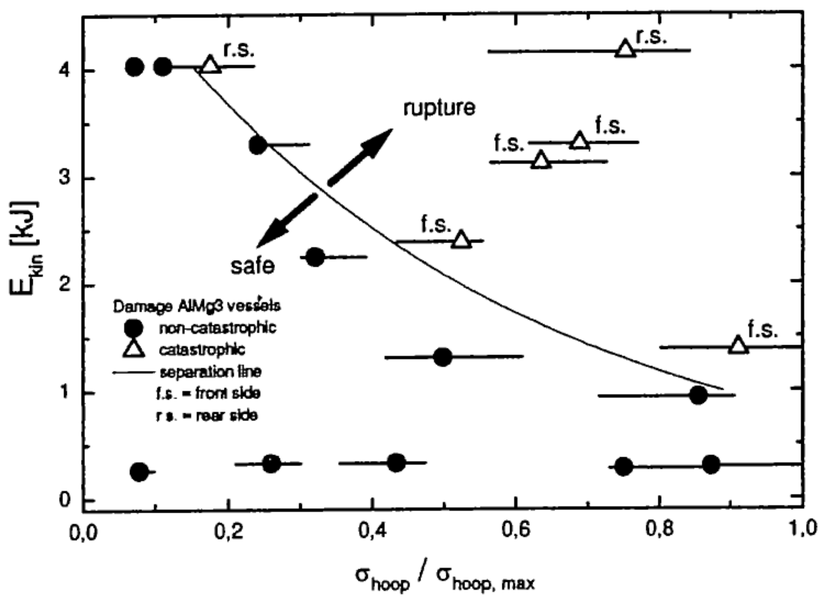

Figure 13 a. Experimental results from hypervelocity impact testing of aluminium pressure vessels

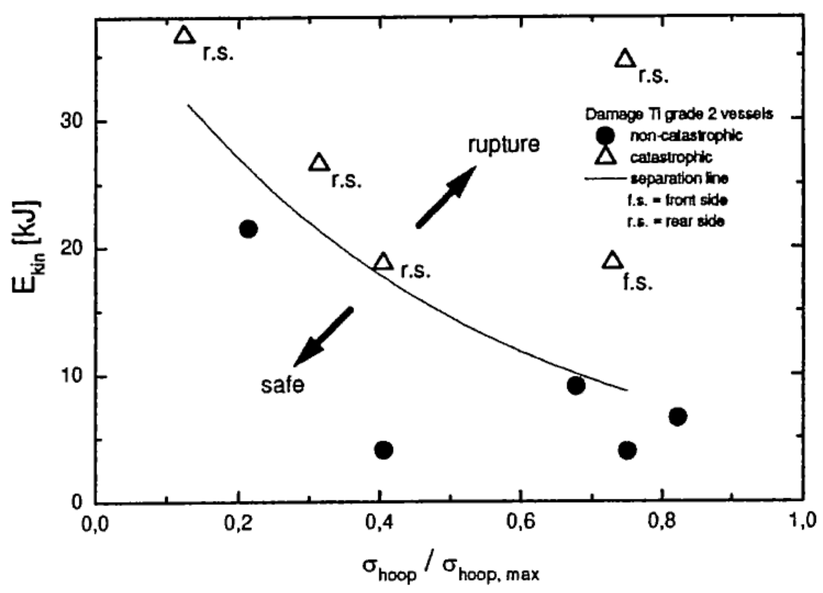

Figure 13 b. Experimental results from hypervelocity impact testing of titanium pressure vessels

parameter regimes has been fit. Experimental parameters taken from below this line result in front wall perforation and different types of non-catastrophic rear side damage, whereas catastrophic rupture occurs for experimental parameters taken from above the curve. The validity of this line is restricted to the presented vessel geometries, materials, stress ranges, and impact velocities in the upper hypervelocity regime around 7 km/s. It is important to understand that this separation line has not been derived from physical laws.

Fig. 14 is a logarithmic plot of all unshielded aluminium and titanium experiments. It is clearly visible that the separation lines for both materials are almost parallel.

8. DISCUSSION

The damage intensity of the hypervelocity impacted gas-filled pressure vessels presented in this study is governed by vessel material, pressure level and impactor energy. Experimental parameters that induce catastrophic rupture were identified. In terms of projectile energy, the resistance to catastrophic rupture is one order of magnitude better for titanium vessels in comparison to aluminium vessels. An empirical curve that separates catastrophic from non-catastrophic parameters is provided as a function of relative wall stresses and kinetic energy. The amount of projectile energy needed to induce catastrophic failure is small at pressures close to the reference burst pressure. At lower pressures, corresponding energies are higher. As an

example, for a relative stress of 0.2, the amount of energy needed to burst an aluminium vessel is 4 kJ, whereas it is around 30 kJ for titanium vessels. At relative stresses of 0.5, corresponding impactor energies amount to about 2 kJ and 15 kJ for aluminium and titanium vessels, respectively.

It was shown that vessel break-up can occur from the front side, driven by stress concentration around the impact hole. In most experiments at pressures exceeding a few atmospheres, the fragment cloud was completely ablated, resulting in no rear wall impact damages. At high pressures and large impact energies however, new mechanisms govern the damage process: a strong gas-shockwave severely bulges the rear wall, and can result in rear side failure.

In the frame of this study, similar damages were identified for aluminium and titanium pressure vessels at corresponding relative wall stresses.

Yet not enough data exist to provide a comprehensive picture of the performance of a shield placed in front of the pressure vessels. In 3 of the 4 investigated cases, shielding prevented burst. As a consequence of the large impact hole in the vessels front wall, the air exhausted quickly, reducing the wall stresses and thus the crack driving force. Thus, the generation of a large impact hole proved to be a favourable side-effect for the prevention of catastrophic bursting.

9. CONCLUSIONS

This study showed that pressure vessels attached to spacecraft bear the potential to rupture catastrophically under impact of a space debris particle.

A simple countermeasure for the prevention of catastrophic bursting is the reduction of wall stresses, i.e. the working pressure. Shielding proved to be very effective for aluminium and titanium vessels, and allows to operate the pressure container at high pressures safely. However, the effect of a shield has to be further investigated, as well as other possible countermeasures.

If catastrophic rupture occurs, wall fragments are ejected at considerable velocities. Even though these velocities are well below the impact velocities of the projectile, large amounts of kinetic energy are involved. It is well known from military research that the penetration potential of such impactors is high. Despite the threat to nearby spacecraft components, large space debris is generated.

10. ANNEX

No.	Experimental parameters					Damage
	d [mm]	v [km/s]	E_{kin} [J]	p [bar]	σ/σ_{max}	rupture [type†]
Al-1	2.0	$6.7^{\pm 0.2}$	260	2.0	0.08	no
Al-2	2.0	7.5	320	6.0	0.23	no
Al-3	2.0	7.5	320	10	0.39	no
Al-4	2.0	6.9	270	19.2	0.75	no
Al-5	2.0	7.1	290	24.6	0.96	no
Al-6	3.0	7.1	930	19.1	0.75	no
Al-7	3.5	6.7	1300	12.7	0.50	no
Al-8	3.5	6.9	1380	23.0	0.90	yes [f.s.]
Al-9	4.1	6.6	2240	8.4	0.33	no
Al-10	4.1	6.8	2380	11.7	0.46	yes [f.s.]
Al-11¶	4.1	7.0	2520	13.0	0.51	yes [r.s.]
Al-12¶	4.4	7.2	3200	6.7	0.26	yes [r.s.]
Al-13	4.4	7.3	3290	ca. 7.9	0.31	no
Al-14	4.4	7.1	3120	15.6	0.61	yes [f.s.]
Al-15	4.4	7.3	3290	16.0	0.63	yes [f.s.]
Al-16	4.9	6.9	4030	1.8	0.07	no
Al-17	4.9	6.9	4030	2.9	0.11	no
Al-18	4.9	6.9	4030	4.3	0.17	yes [r.s.]
Al-19	4.9	7.0	4150	18.3	0.71	yes [r.s.]

† f.s.: front side; r.s.: rear side

¶ experiments failed

Table 1 Experimental parameters of hypervelocity impact tests on aluminium pressure vessels

No.	Experimental parameters					Damage
	d [mm]	v [km/s]	E_{kin} [J]	p [bar]	σ/σ_{max}	cat. burst [type†]
Ti-1	5.0	6.9	4020	30.3	0.41	no
Ti-2	5.0	6.8	3910	56.0	0.75	no
Ti-3	6.0	6.6	6510	61.4	0.82	no
Ti-4	7.0	6.1	9020	50.6	0.68	no
Ti-5	8.0	7.5	21900	ca.16	0.21	no
Ti-6	8.0	7.0	19100	30.2	0.40	yes [r.s.]
Ti-7	8.0	7.0	18100	54.4	0.73	yes [f.s.]
Ti-8	8.9	7.1	26000	23.4	0.31	yes [r.s.]
Ti-9	10.0	7.0	36000	9.3	0.12	yes [r.s.]
Ti-10	10.0	6.8	33500	55.7	0.75	yes [r.s.]

† f.s.: front side; r.s.: rear side

Table 2 Experimental parameters of hypervelocity impact tests on titanium pressure vessels

No.	Experimental parameters					Damage
	d [mm]	v [km/s]	E_{kin} [J]	p [bar]	σ/σ_{max}	cat. burst
Al-20	5.0	6.4	3490	10.7	0.42	no
Al-21	6.0	5.7	4860	11.1	0.43	no

Table 3 Experimental parameters of hypervelocity impact tests on shielded aluminium pressure vessels

No.	Experimental parameters					Damage
	d [mm]	v [km/s]	E_{kin} [J]	p [bar]	σ/σ_{max}	cat. burst
Ti-11	8.0	7.2	20200	30.5	0.41	no
Ti-12	10.0	6.8	34000	61.4	0.82	yes

Table 4 Experimental parameters of hypervelocity impact tests on shielded titanium pressure vessels

11. ACKNOWLEDGEMENT

This study was performed under contract of the European Space Agency ESA.

12. REFERENCES

1. Results from Post-Flight Investigation of the Retrieved HST Solar-Array, *Proceedings of the Hubble Space Telescope Solar-Array Workshop*, ESA-ESTEC, Noordwijk, The Netherlands, May 30-31, 1995

2. Whitney, J. P., and White, P. D., Designing Hypervelocity Impact Testing for Thin-Walled Pressure Vessels, Presented at the *43rd Meeting of the Aeroballistics Range Association*, Columbus, Ohio, 1992

3. Whitney, J. .P., Hypervelocity Impact Tests of Shielded and Unshielded Pressure Vessels, *NASA Johnson Space Center*, JSC 32294, 1993

4. Friesen, L. J., Hypervelocity Impact Tests of Shielded and Unshielded Pressure Vessels, Part II, *NASA Johnson Space Center*, JSC 27081, 1995

5. Schonberg, W. P., Characterizing the material in a debris cloud created in a hypervelocity impact, *Proceedings of the First European Conference on Space Debris*, ESA SD-01, Darmstadt, Germany, April 5-7, 1993

6. Piekutowski, A. J., Formation and Description of Debris Clouds Produced by Hypervelocity Impact, *NASA Contractor Report* No. 4707, Marshall Space Flight Center, Alabama, USA, 1996

7. Schäfer, F., Schneider, E., Lambert, M., and Mayseless, M., Propagation of a Hypervelocity Impact Fragment Cloud in Pressure Gas, to be published in *Int. J. Imp. Engng*, in press

8. Weidmann, G., Lewis, P., and Reid, M., Structural Materials, Materials in Action Series, *The Open University*, Butterworth-Heinemann Ltd, Oxford, Great Britain, 1990

9. Welsch, G., Boyer, R., and Collings, E. W., Material Properties Handbook: Titanium Alloys, *ASM International*, Materials Park, Ohio, USA, 1994

10. Crozier, W. D., and Hume, W, High Velocity Light Gas Gun, *J. of Appl. Phys.*, Vol. 28, 1957

11. Stilp, A., Review of Modern Hypervelocity Impact Facilities, *Int. J. of Impact Engng.*, Vol. 5, 613-621, 1987